Soil Biology and Biochemistry 182 (2023) 109041

Contents lists available at ScienceDirect

Soil Biology and Biochemistry

journal homepage: www.elsevier.com/locate/soilbio

Warming, permafrost thaw and increased nitrogen availability as drivers for plant composition and growth across the Tibetan Plateau

Hanbo Yun [a,b,c,**], Qing Zhu [d], Jing Tang [b,e,f], Wenxin Zhang [b,e], Deliang Chen [g], Philippe Ciais [h], Qingbai Wu [a], Bo Elberling [b,*]

[a] State Key Laboratory of Frozen Soil Engineering, Beilu'He Observation and Research Station on Tibetan Plateau, Northwest Institute of Eco-Environment and Resources, Chinese Academy of Sciences, 730000, Lanzhou, Gansu, China
[b] Center for Permafrost (CENPERM), Department of Geosciences and Natural Resource Management, University of Copenhagen, DK1350, Copenhagen, Denmark
[c] Department of Earth, Atmospheric, and Planetary Sciences, Purdue University, 47906, West Lafayette, Indiana, USA
[d] Climate Sciences Department, Climate and Ecosystem Sciences Division, Lawrence Berkeley National Laboratory, 94720, Berkeley, California, USA
[e] Department of Physical Geography and Ecosystem Science, Lund University, SE-22362, Lund, Sweden
[f] Department of Biology, Terrestrial Ecology, University of Copenhagen, DK-2100, Copenhagen, Denmark
[g] Department of Earth Sciences, University of Gothenburg, 41320, Gothenburg, Sweden
[h] IPSL – LSCE, CEA CNRS UVSQ UPSaclay, Centre D'Etudes Orme des Merisiers, 91191, Gif sur Yvette, France

ARTICLE INFO

Keywords:
Nitrogen
Permafrost thawing
Climate warming
Tibetan plateau

ABSTRACT

Permafrost-affected ecosystems are subject to warming and thawing, which can increase the availability of subsurface nitrogen (N) with consequences in otherwise N-limited tundra and alpine vegetation. Here, we quantify the extent of warming and permafrost thawing and the corresponding effects on nitrogen availability and plant growth based on a 20-year survey across 14 sites on the Tibetan Plateau. The survey showed that most sites have been subject to warming and thawing and that the upper permafrost zone across all sites was rich in inorganic N, mainly as ammonium. We further explore the efficiency of plants to utilize ^{15}N-labelled inorganic N over five years following ^{15}N addition at the permafrost table far below the main root zone. The ^{15}N experiment showed that deep-rooted plant species were able to utilize the labelled N. A SEM model suggests that changes in vegetation can be explained by both active layer warming and permafrost thawing and the associated changes in inorganic nitrogen availability. Our results highlight a feedback mechanism of climate warming, in which released plant-available N may favour deep-rooted plants. This can explain important changes in plant composition and growth across the sites on the Tibetan Plateau.

1. Introduction

Permafrost underlies about 25% of the land surface in the Northern Hemisphere (Obu et al., 2019) and the area has recently warmed more than twice as much as the rest of the planet (Parmesan et al., 2022). Such warming is expected to change both carbon sinks and resources of the permafrost-affected ecosystems, and thereby impact the net carbon–climate feedback on a global scale (Virkkala et al., 2021; Bjorkman et al., 2018; Niittynen et al., 2018). It has been suggested that plant community composition and plant growth have significantly changed in permafrost-affected ecosystems and that changes are associated with both the organic and the inorganic nitrogen cycle, for instance, through thawing permafrost, which can release nitrogen (N) previously held in frozen soil layers (Elberling et al., 2010; Keuper et al., 2017; Salmon et al., 2018). These changes can affect the N availability for plants (Kou et al., 2020; Hewitt et al., 2019; Pedersen et al., 2020), and induce changes in plant growth, competition and plant succession (Heijmans et al., 2022).

Air temperature (Niittynen et al., 2018; Elmendorf et al., 2012), soil moisture (Heijmans et al., 2022; Elmendorf et al., 2012; Happonen et al., 2022) and nutrition (Niittynen et al., 2018; Elmendorf et al., 2012; Schuur et al., 2007; Myers-Smith et al., 2019) are all considered

* Corresponding author. Center for Permafrost (CENPERM), Department of Geosciences and Natural Resource Management, University of Copenhagen, DK1350, Copenhagen, Denmark.
** Corresponding author. State Key Laboratory of Frozen Soil Engineering, Beilu'He Observation and Research Station on Tibetan Plateau, Northwest Institute of Eco-Environment and Resources, Chinese Academy of Sciences, 730000, Lanzhou, Gansu, China.
E-mail addresses: hbyun@lzb.ac.cn (H. Yun), qbwu@lzb.ac.cn (Q. Wu), be@ign.ku.dk (B. Elberling).

https://doi.org/10.1016/j.soilbio.2023.109041
Received 22 January 2023; Received in revised form 16 April 2023; Accepted 18 April 2023
Available online 29 April 2023

important factors for plant growth and plant composition in permafrost-affected ecosystems. However, these factors reveal a high spatiotemporal heterogeneity in permafrost-affected ecosystems (Elberling et al., 2010; Salmon et al., 2018; Heijmans et al., 2022), which complicates the understanding and quantification of mechanisms and drivers of observed changes (Niittynen et al., 2018; Myers-Smith et al., 2019). This is particularly true when scaling observations across permafrost biomes and longer time scales (Bjorkman et al., 2018; Thomas et al., 2020).

The Tibetan Plateau accounts for 75% of the Northern Hemisphere's alpine permafrost area and has experienced significant climate and environmental changes in recent decades (Chen et al., 2015; Yao et al., 2019; Ehlers et al., 2022). Future warming has been predicted to result in an increase in active layer thickness up to 3.3 m (Zou et al., 2017) and an increase in the length of plant root (Liu et al., 2018), and approximately 1.9 Pg and 3.8 Pg C release from permafrost by 2100 under RCP 4.5 and 8.5, respectively (Wang et al., 2020). Here, we hypothesize that nitrogen released as a result of permafrost thaw has been available in mainly deep-rooted plant species and that this, in combination with N release associated with active layer warming, has resulted in changes in both plant community composition and plant growth.

We undertook two steps to quantify links between permafrost conditions and plant species composition and growth across the Tibetan Plateau. We first quantified the plant uptake of labelled nitrogen (^{15}N) introduced at the permafrost table for five years. Secondly, we quantified plant species composition and plant growth based on the maximum rooting depth, plant coverage, plant height and aboveground biomass in September and climate data linked to active layer warming, permafrost thaw and changes in plant nutrient availability. Data were collected from 14 sites across the Tibetan Plateau (Fig. 1) between 1975 and 2017 and included 1838 soil cores from 692 plots and corresponding plant species and root depth.

2. Methods

2.1. Meteorological data

Air temperature, air humidity, soil temperature, soil moisture and total precipitation were obtained from the China meteorological data service centre (http://data.cma.cn/) and the State Key Laboratory of Frozen Soil Engineering, China (SKLFSE, http://sklfse.nieer.ac.cn/; for details, see SI.1.1). Maximum active layer thickness (ALT) was calculated based on the 0 °C isotherm for soil temperature profiles and growing degree days (GDD) were calculated according to Bendixen et al. (2017).

2.2. Stable isotope N addition experiment

Labelled ^{15}N was added to the permafrost table and subsequently followed in plants at six sites from 2017 to 2021. At each site, labelled N (1 g ^{15}N–NH_4CI, 99 atom%) was dissolved in 50 g deionized water and added at the permafrost thaw front by a sloping drill hole (SI.1.2). The ^{15}N addition was made in five replicate plots per site. The aboveground biomass (including leaves and stems) as well as roots within the upper 50 cm were collected within an area of 33 cm × 33 cm above the injection point. Plant species included three dominating species: *Carex moorcroftii* Falc. Ex Boott (Carex), *Kobresia littledalei* C. B. Clarke (Kobresia) and *Oxytropis pauciflora* Bunge (Oxytropis). Four mature individual plants were randomly selected for each species and the belowground biomass was sampled by using a soil drill with a diameter of 15 cm. Collection also took place in five additional control plots per site (without labelled N being added). Roots and plants were collected about ten days, one year, two years, three years, and four years after the addition (SI.1.2).

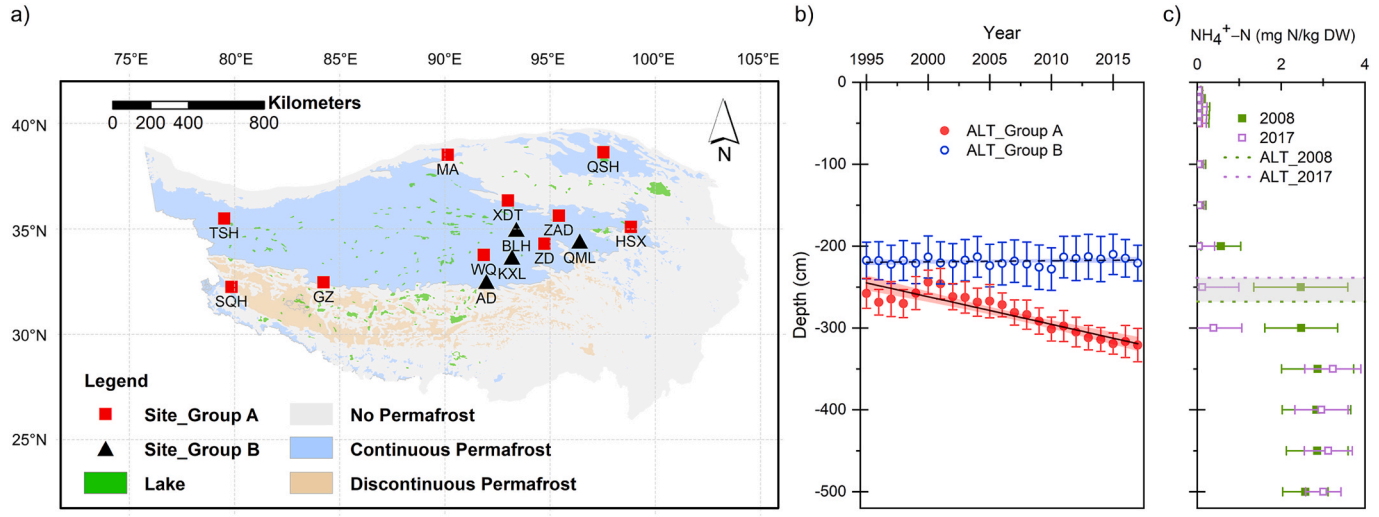

Fig. 1. **a**. Map of sampling sites on the Tibetan Plateau (TSH: TianshuiHai; QSH: QingshuiHe; SQH: ShiqianHe; GZ: GaiZi; MA: MangAi; AD: AnDuo; WQ: Wen Quan; KXL: KaixinLing; BLH: BeiluHe basin; ZAD: ZaDuo; XD: XidaTan; ZD: ZhiDuo; QML: QumaLai; HSX: HuashiXia). The boundaries of the Tibetan Plateau area and permafrost distribution are based on Zou et al. (2017). Panel **b** shows the variations in active layer thickness (ALT) from 1995 to 2017 for group A (red solid dot) and group B (blue open circle), respectively. The black solid line denotes a significant change ($p < 0.05$), whereas the black dashed line indicates no significant change ($p > 0.05$). Vertical bars represent one standard deviation, n = 265 for group A and n = 88 for group B. Blue and red ribbons denote 95% confidence intervals. Panel **c** shows NH_4^+ profiles of 14 sites sampled at the end of September in 2008 and in 2017 (horizontal bars representing one standard deviation, n = 640). Green and purple dashed lines are the mean thickness of the active layer (ALT) across sites for 2008 and 2017, respectively. The grey region denotes the variation of permafrost thaw front from 2008 to 2017.

2.3. Collection of soil, permafrost and plant samples

Soil and permafrost cores were taken as two pseudo-replicate cores within the same vegetation type at 14 sites (Fig. 1) and sampled in 1975 and 1978 and annually from 1995 to 2017 (26 years). At nine sites (AD, QML, BLH, HSX, TSH, SQH, ZD, MA and GZ), 1078 cores from 62 plots were studied in 1975 and 1978 and from 1995 to 2017 (26 years). At five sites (WQ, QSH, KXL, ZAD and XD), a total of 760 cores from 96 plots were studied from 2002 to 2017 (16 years). At all sites, samples 0–100 cm deep were collected using a soil corer at the following depths: 0–5 cm, 5–10 cm, 10–15 cm, 15–20 cm, 20–30 cm, 30–40 cm, 40–50 cm, 50–100 cm. A motorized drill was used to collect samples at 50-cm intervals between 1 and 5 m. Samples were collected using a stainless steel ring cutter, with three replicates. All samples were marked and sealed in 100-ml steel aluminium boxes, weighed, frozen at −15 °C, and brought back to the laboratory to be used for soil analysis.

At each site, we randomly selected a 100 m transect for vegetation investigation within a 500 m radius of the permafrost soil temperature monitoring borehole. Along the 100 m transect, we randomly placed five pairs of plots. One side of each plot, measuring 1.5 m × 1.5 m, was used for the collection of plant species-specific root length, while the other side, measuring 1 m × 1 m, was used for the collection of plant coverage, plant height and total biomass (i.e., aboveground biomass including all species). For each pair of plots, additional information including landscape type, surface drainage and erosion status was noted. Plant coverage was measured in early or mid-September at five plots (1 m × 1 m) within 500 m from where the soil and permafrost cores had been collected. In 1975 and 1978, it was estimated based on observations by experts. From 1995 to 2007, the pin-point method was applied to quantify plant coverage. This method was based on a 10 cm × 10 cm nylon mesh placed over a 1 m × 1 m plot. From 2008 to 2017, a US agricultural multispectral camera was used to quantify plant coverage. A comparison of the two methods to quantify plant coverage revealed no significant differences.

The aboveground biomass was quantified in three 20 cm × 20 cm subplots within each plot during September, in a total of 15 subplots per site. At each subplot, aboveground biomass was cut using scissors, packed in paper bags and returned to the laboratory. Here, any soil particles on plants were removed prior to plant samples being dried at 75 ± 2 °C for 72 h to calculate the aboveground biomass. In these calculations, grazing was not accounted for as all sites were fenced off for the duration of the experiment to avoid grazing by yaks or other large wild animals.

To investigate the root vertical distribution pattern of the plant species in the community, a 1.5 m deep pit was dug in five 1.5 m × 1.5 m quadrats to measure the maximum root depth after all of the above work was finished. Since 2008, this approach has been replaced by a special soil-sample drilling device (of 15 cm diameter) designed by SKLFSE, China. The vertical root distribution was based on fresh roots being observed in soil cores (after cores have been soaked in water) in three replicates per plot. A mean value was calculated for the maximum root per plot. Additional deep soil profile samples were collected in areas with retrogressive thaw slumps near study sites (see SI.1.3).

2.4. Chemical analysis

The following analyses were undertaken for each soil depth and at each time point. Soil bulk density and soil water content were estimated as the change in mass after drying in a volume-specific soil sample. Soil pH was determined by amperometry (DJS–1C, Leizi, Shanghai, China). Five grams of fresh soil were mixed with $CaCl_2$ (0.2 M) at a ratio of one part soil to five parts liquid (1:5), and the pH of the suspension was measured after 1 h of shaking for each soil sample. Soil organic carbon (SOC) of the air-dried soil samples was analysed using the wet combustion method, Walkley–Black modified acid dichromate digestion, $FeSO_4$ titration and an automatic titrator (Yun et al., 2018; Wu et al., 2016). Total nitrogen (TN) was titrated by the Kjeldahl method (Wu et al., 2016) before the year 2000, and since 2001, it has been measured by an elementary analyser (Vario EL Three, Elementar, Germany). Nitrate (NO_3^-) was measured by capacity titration (ELIT 8021, Beijing, China) before the year 2000, and afterwards by ion chromatography (T6–New Century Spectrophotometer, PUXI, Beijing, China).

Soil ammonium (NH_4^+) content was analysed based on soil samples collected from 2008 to 2017. Ammonium was extracted using a 2 M potassium chloride (KCI) solution in a 1:5 ratio (soil and solution) for 2 h and subsequently quantified using a flow injection analyser (Auto-analyser 3 SEAL, Bran and Luebbe, Norderstedt, Germany) with a detection limit of 0.003 N mg L^{-1}. The NH_4^+ concentration was calculated as mg N kg^{-1} dry weight (DW) of soil.

Grounded root samples (0.2–0.3 mg) were folded into tin capsules and analysed for ^{15}N on a Costech ECS 4010 Elemental Analyser (Costech ECS4010, Italy), which was coupled to a Thermo Finnigan MAT 253 continuous flow isotope-ratio mass spectrometer (Thermo Scientific, Bremen, Germany).

Soil property data and plant data were provided by the SKLFSE, China and the National Cryosphere Desert Data Centre, China (http://www.ncdc.ac.cn/portal/. Data quality control and analysis are described in detail (SI.1.4).

Structure equation model (SEM). A piecewise SEM was examined to identify 1) the pathway of plant growth potentially affected by climate change; 2) the difference between the direct and indirect effects of temperature, water balance and soil nutrients on plant growth. The mean value at the level of a site in the growing season was used in SEM analysis and split into two groups, A and B. The SEM included the following drivers: air temperature at 2 m, growing degree days, soil temperature at 0–50 cm, soil temperature at 50–100 cm, ALT, soil moisture at 0–50 cm, soil temperature at 50–100 cm, soil N–NO_3^- concentration at 0–50 cm, soil N–NO_3^- concentration at 50–100 cm, NO_3^- concentration at 100 cm-permafrost table, N–NH_4^+ concentration at 0–50 cm, N–NH_4^+ concentration at 50–100 cm, and N–NH_4^+ concentration at 100 cm-permafrost table. Variations in soil nutrients were assumed to be dominated by variations in total nitrogen, whereas variations in ammonium (NH_4^+) were used as an indicator of nitrogen released from permafrost (see Supplementary information SI.1.14 for justification for this assumption).

All variables were standardized using *z*-scores (mean zero, unit variance). Principal component analysis (PCA) was then used to summarize the structure between plant growth and environmental drivers for plant growth. We assumed linear Gaussian relationships between variables included in the model, after a normality test with density plots for each variable (Grace, 2006).

Due to the concern of a time lag between nitrogen being released from permafrost thaw and the effects on plants, we fitted separate models window-by-window from 0 to 5 years both for the growing season and for the non-growing season. This approach (see details SI.1.4) was used to 1) test whether a time lag of 1–2 years in SEM was an

artefact setting and 2) account for possible time lag effects of climate change variables (i.e., non-growing season air temperature and soil temperature). In the final SEM, plant uptake of nitrogen released from permafrost was assessed with a two-year time lag. Thus, the final soil-permafrost nitrogen dataset covered the period from 1995 to 2015 while the climate and plant dataset included data from 1997 to 2017.

Skill diagnostics. The goodness of fit of SEMs was estimated by chi-square (χ^2), degrees of freedom (*d.f.*), and root-mean-square error of approximation (RMSEA). A path coefficient was used to indicate the sign and strength of the relationships between two variables, which is analogous to the partial correlation coefficient or regression weight (R^2; Mallet, 1986). The standardized total effect was calculated to quantify the contribution of all drivers to plant growth (r^2). The net influence that one variable had upon another was calculated by summing all direct and indirect pathways (effects) between two variables. All SEM analyses were conducted using the piecewise SEM R package.

3. Results

3.1. Soil and permafrost characteristics

Climate data show that the mean annual air temperatures (MAATs) ranged from −4.2 to 0.8 °C from the northern to southern sites across the Tibetan Plateau, and have significantly increased from 1975 to 2017 ($p < 0.05$; Fig. S1). Annual precipitation ranged from 83.0 to 460.0 mm across sites in the study area and changes in precipitation occurred mainly during the non-growing season (Fig. S2). The mean soil temperature at 0–100 cm depth was −2.5 ± 1.7 °C, and the mean soil water content (SWC) at 0–100 cm depth was 12.0 ± 5.3% (Fig. S3). Although air temperature increased between 1975 and 2017, soil temperatures at 0–100 cm depth showed different responses (Fig. S3). SWC of the 0–100 cm layer did not show significant changes at most sites, except for sites AD and KXL, which showed a significant increase during the study period. In this study, the mean active layer thickness (ALT) between 1975 and 2017 was 248.0 ± 38.0 cm, and has increased on average at a rate of 20.2 ± 4.6 cm per decade (Fig. S4). The maximum increase in ALT was observed at site QSH (35.8 cm per decade; Fig. S5), which is a relatively dry, well-drained site with low ice content at the top of the permafrost (data not shown). Based on observed ALT trends from 1975 to 2017, the 14 study sites were split into group A with significantly positive increasing trends, consisting of TSH, QSH, SQH, GZ, MA, WQ, ZAD, XD, ZD, HSX, and group B without significant changes consisting of AD and BLH and with significantly negative trends consisting of KXL and QML (Fig. S5). These two groups are hereafter used for further analyses.

During the study period, on average 83% of the roots were found within 0–50 cm, 16% within 50–100 cm, and 1% below 100 cm. Consequently, the active layer in the following is discussed for each of these three depth intervals (0–50 cm, 50–100 cm, and 100 cm–permafrost table). From 1995 to 2017, the soil bulk density was around 1.81 g cm^{-3} at 0–50 cm, 50–100 cm and 100 cm–permafrost tables both in group A and group B. For group A sites, a significant change was noted in two depth intervals: 0–50 cm and 50–100 cm, but no significant changes were observed in the deeper layer or any depth intervals for group B sites (Fig. S6 a and b). A *t*-test showed that the three layers did not reveal any significant differences between groups A and B. Taking the depth-specific soil bulk density and the soil organic carbon (SOC) concentration into account, SOC stock at 0–50 cm showed a significant decrease ($p < 0.01$) with a rate of 0.08 kg C m^{-2} y^{-1} during 1995–2017 in group A (Fig. S7 a). In total, 31% of the SOC within the top 50 cm has been mineralized within the last 20 years at group A sites; however, changes in SOC stock were not significant at deeper depths (Fig. S7 a). For the group B sites, SOC stocks (0–50 cm, 0–100 cm and 0 cm–permafrost table) revealed no significant changes (Fig. S7 b). Decomposition at 0–50 cm within group A sites did not result in any significant changes in soil pH (Fig. S6 g) nor in any other depth intervals in group A or B sites (Fig. S6 h).

The total nitrogen (TN) stock for the group A sites in the upper 0–50 cm layer significantly decreased ($p < 0.01$); in the 0–100 cm layer it decreased as well ($p = 0.055$), but in the entire active layer (0 cm to permafrost table) it significantly increased during 1995–2017 ($p < 0.01$; Fig. 2 and S7 c). For the group B sites, TN stock of the 0–50 cm, 0–100 cm and entire active layer did not change significantly (Supplementary Fig. S7 d). The mean carbon-to-nitrogen ratio (C/N) of 0–100 cm was 10.71 ± 2.35 for group A, which significantly increased during 1995–2017 (ranging from 8.82 ± 1.01 to 13.93 ± 1.78; Fig. S7 e), and for group B, C/N of 0–100 cm was 10.42 ± 1.75 (ranging from 9.52 ± 1.55 to 11.61 ± 2.66), showing no significant change during the same period (Fig. S7 f).

3.2. Release of nitrogen from thawing permafrost and uptake by plant

Soil-permafrost cores collected from 2008 to 2017 show that the ammonium (NH_4^+) concentration extracted from permafrost samples (up to 500 cm below the surface) was approximately 100 times higher than samples in the active layer (AL) for both groups A and B (Fig. 1c). These observations highlighted that, upon thawing, permafrost can potentially be an important source of NH_4^+ for plant growth if accessible via plant roots. This motivated a controlled ^{15}N addition at the permafrost table, which is described below.

A stable isotopic labelling (^{15}N–NH_4^+) experiment was conducted during 2017–2021 to explore whether NH_4^+ released at the permafrost table in autumn is accessible for plants. The investigation included both deep-rooted species and shallow-rooted species. Our ^{15}N–NH_4^+ addition experiment demonstrated that even by one year after addition, above-ground plant tissue has a significant enrichment of labelled N (Fig. 3). For group A sites with significant warming and permafrost thawing, the ^{15}N enrichment values increase to more than 200 $\mu g^{15}N$ gN^{-1} in subsequent years, whereas for group B sites the enrichment values increased to 2–6 $\mu g^{15}N$ gN^{-1} depending on the plant species (Fig. 3). It is worth noting that in the experiment, ^{15}N-labelled nitrogen was only supplied as ammonium. However, because ammonium can be converted to nitrate through nitrification, it is not possible to conclude here if plants have incorporated permafrost N as ammonium or as nitrate. The observations highlight the potential for deep-rooted species to benefit from permafrost-released N compared to shallow-rooted species.

3.3. The link between nitrogen dynamics and plant growth

Long-term trends in biologically available N and plant biomass were used to assess the links between N dynamics driven by climate change and plant growth. There were 85 graminoids and two deciduous dwarf shrubs (*Potentilla parvifolia* Fisch. ex. Lehm. and *Myricaria prostrata* Hook. f. et Thoms. ex Benth.) recorded in group A (Table ST1). The mean species richness increased from 15.5 species m^{-2} (1995) to 23.8 species m^{-2} (2010; $p < 0.1$) and then declined to 18.5 species m^{-2} (2017; $p < 0.05$; Fig. 2; Fig. S9 a). There were 62 graminoid species and one dwarf

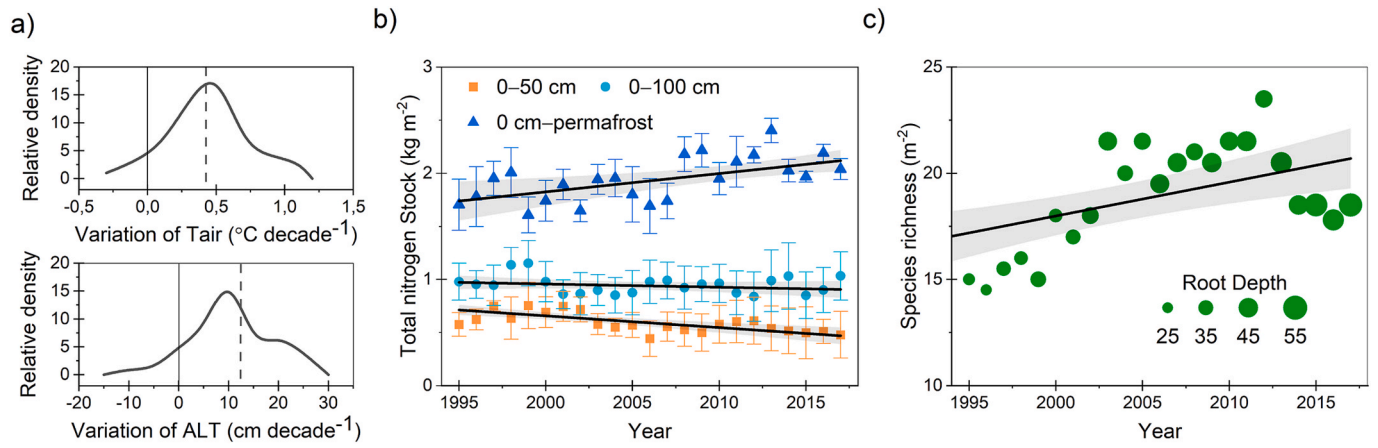

Fig. 2. Changes in climate, total soil nitrogen stock (TN) and species richness in group A sites from 1995 to 2017. **a**) Air temperature (Tair) and active layer thickness (ALT), with the vertical solid grey lines indicating the zero line and the colour-dashed lines showing the mean value. **b**) Changes in TN stock in three depth intervals: 0–50 cm, 0–100 cm and 0 cm–permafrost. Solid black lines represent regression lines (p-value <0.05), and the grey regions represent the 95% confidence intervals from the predicted line of TN stock over time. **c**) Changes in plant species richness and vertical root distribution. The solid black line represents a significant change over time ($p < 0.05$) and the grey region represents the 95% confidence interval from the predicted line of species richness (m^{-2}) over the period 1995 to 2017.

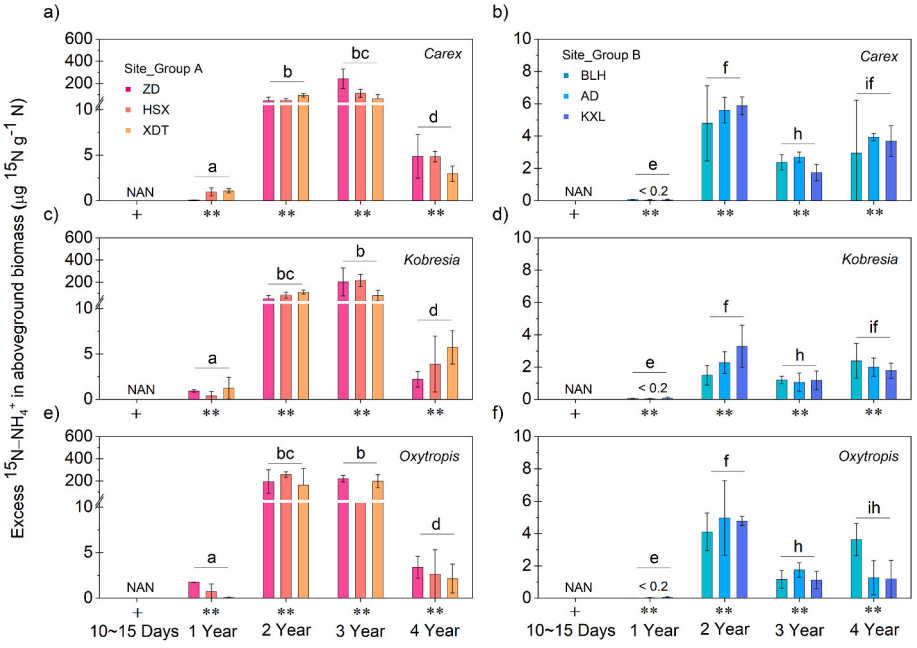

Fig. 3. Plant ^{15}N–NH_4 uptake (excess ^{15}N–NH_4 concentration in plant leaves and stem) after 10–15 days, 1 year, 2 years, 3 years and 4 years in four deep–rooted plant species in group A (**a**, **c**, **e**) and group B (**b**, **d**, **f**). **a** and **b** were *Carex moorcroftii* Falc. Ex Boott (*Carex*), **c** and **d** were *Kobresia littledalei* C. B. Clarke (*Kobresia*), and **e** and **f** were *Oxytropis pauciflora* Bunge (*Oxytropis*). Vertical bars represent one standard deviation, n = 15 (after 1 year, n = 12). NAN indicates values were below the detection limit. The ** on the x-axis indicates that the ^{15}N–NH_4 uptake was significant as compared to initial values, while + indicates no significant difference ($p > 0.05$). Lowercase letters indicate significant differences ($p < 0.05$) between sampling times.

deciduous shrub (*Myricaria prostrata* Hook. f. et Thoms. ex Benth.) in group B (Table ST2), and no temporal trends were observed (with mean species richness of 16.1 m^{-2}; Supplementary Fig. S9 b). During the period 1975–2017, maximum root depth significantly increased from 66.8 ± 15.2 cm to 103.7 ± 17.4 cm in group A (Tables ST1), whereas no significant change (from 62.7 ± 6.7 cm to 75.6 ± 5.1 cm) was noted for group B (Tables ST2). Specific species' root depths were not sampled for all known plant species during the study period. However, the maximum root depths of four plant species known to have long roots were quantified in selected sites in both groups A and B (Fig. 4). For these four plant species, the maximum root depth increased significantly. For instance, *Astragalus melanostachys* roots changed from 52.1 ± 5.9 cm in 1995 to 69.7 ± 5.3 cm in 2017 at group A sites, but no significant change was observed at group B sites (Fig. 4c). Furthermore, convergent crossing mapping (CCM) was conducted between the variation of maximum root length and variation of nitrogen at 50–100 cm depth, which showed a positive correlation during the period 1995–2017. The CCM results suggest that variations in soil nitrogen at 50–100 cm appear to be a stronger driver for changes in maximum root length than an increase in the root growth is a driver for the soil nitrogen content in the same depth interval (Fig. S10).

Subsequently, we compared the annual aboveground biomass in September between group A and group B from 1995 to 2017 (Table ST3). The mean aboveground biomass for September was 234.5 ± 8.0 g m^{-2} for group A and 249.4 ± 6.9 g m^{-2} for group B. Though a t-test revealed no significant differences between group A and group B, the aboveground biomass at group A sites increased significantly during 1995–2002 ($p < 0.05$) but decreased significantly during 2003–2012 ($p < 0.01$; Table ST3). For group B, the aboveground biomass did not show any significant changes in the two periods of 1995–2002 or 2003–2012.

Interestingly, from 2008 to 2020 at permafrost thaw sites (group A sites), the plant species-specific results showed no consistent patterns of root length increase or biomass accumulation, either aboveground or belowground, such as at site XD (Fig. S11). For the deep-rooted species,

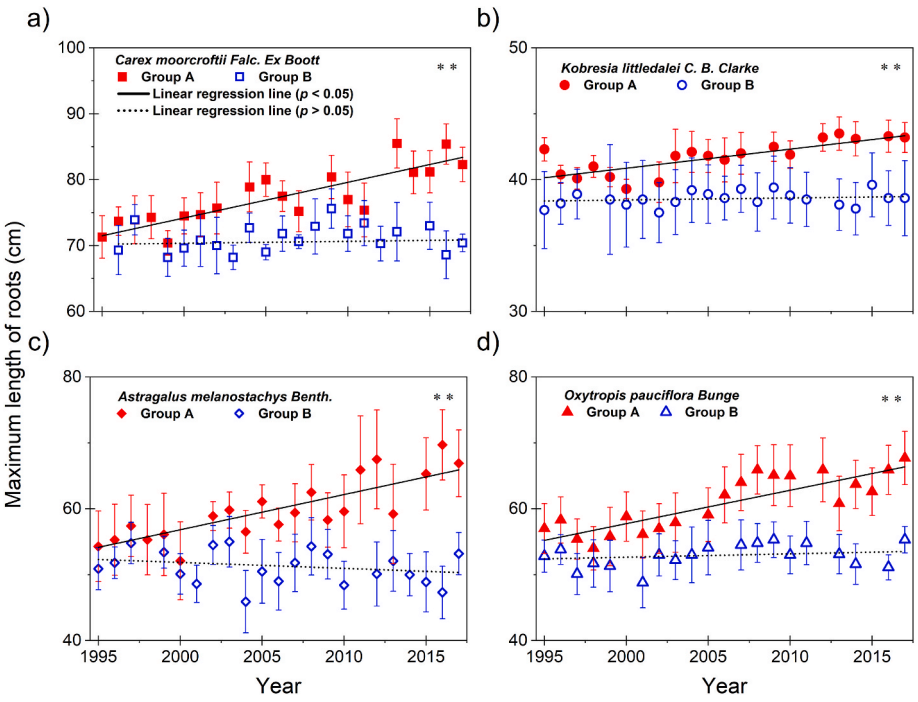

Fig. 4. Changes in maximum length of plant species–specific roots in four deep–rooted species at group A and B sites from 1995 to 2017. **a** is *Carex moorcroftii* Falc. Ex Boott, **b** is *Kobresia littledalei* C. B. Clarke, **c** is *Astragalus melanostachys* Benth., and **d** is *Oxytropis pauciflora* Bunge. Vertical bars represent one standard deviation, n = 4. ** indicate significant differences (p-value <0.05) between group A and group B sites.

Anemone imbricata Maxim. and *Oxytropis glacialis*, root length increased significantly with aboveground biomass increase, while the shallow-rooted species, *Leontopodium pusillum* (Beauv.) Hand. –Mazz. and *Heteropappus bowerii* (Hemsl.) Griers., showed no changes in root length or aboveground biomass. Furthermore, the root length of *Saussurea wellbyi* Hemsl. decreased significantly, while aboveground biomass increased significantly. This result suggests that shallow-rooted species can be affected differently by climate change from deep-rooted species on the Tibetan Plateau. Specifically, shallow-rooted species seem to be able to benefit from increasing near-surface mineralization associated with AL warming, while deep-rooted species significantly increased in both root length and aboveground biomass, which could be due to the increased N availability linked to permafrost thaw.

4. Discussion

4.1. Permafrost nitrogen

In permafrost-affected ecosystems, N acquisition for a plant is mainly restricted to the active layer soil (Blume-Werry et al., 2019; Iversen et al., 2015). The underlying permafrost table is an impermeable barrier that restricts the movement of water and dissolved nutrients (McNamara et al., 1999). But thawing permafrost can be considered a source of N, as top permafrost layers generally consist of a higher concentration of ammonium (NH_4^+) than the active layer above (Hansen and Elberling, 2023). However, plant uptake of N near the permafrost table depends on the form in which N is released and that roots are present to utilize the N source. On the Tibetan Plateau, we report here that permafrost soils predominantly hold inorganic N in the form of NH_4^+ (2–4 mg N kg^{-1} DW) and roughly 100 times higher concentrations than observed in the active layer. In contrast, permafrost nitrate (NO_3^-) concentrations were low. These observations are consistent with observations from the Arctic (Beermann et al., 2017; Elberling et al., 2010; Hansen and Elberling, 2023). However, NH_4^+ has the potential to be converted into NO_3^- via nitrification in the presence of oxygen (Oulehle et al., 2016), but has not been documented in this study. While NH_4^+ has relatively low mobility and is preferred by most plants (Clemmensen et al., 2008), NO_3^- is more soluble and has a higher export potential (Pedersen et al., 2022). Hence, the N-form upon release, N-processes and abiotic transport processes within the soil profile and along hydrological gradients may contribute to determining both the transport potential of N and the temporal-spatial tends in plant access to N in a permafrost-affected landscape.

4.2. Root utilization of permafrost nitrogen

One mechanism by which plants can utilize N released from thawing permafrost is by living root reaching the permafrost table and taking up N at the point of release as suggested by Keuper et al. (2017) for a shallow peatland and Pedersen et al. (2020) for mineral soil with a maximum thaw depth of about 1 m. In the present study, the mean depth to the permafrost table was 248 ± 38 cm (Fig. S4), which makes it more difficult for plant roots to reach the point of N release. However, our stable isotopic labelling (^{15}N–NH_4^+) experiment shows that aboveground plant tissue had a significant amount of labelled N incorporated already one year after the addition of ^{15}N–NH_4^+ at the permafrost table (Fig. 3). As shown, uptake within a year was only significant for plant species known to have long roots and observed to have live roots reaching at least 2.4 m (SI 1.3.) below the surface.

We show that plants have been able to utilize nitrogen being added to an average depth of 3.3 m below the surface (mean thickness of the maximum active layer) and even as deep as 3.6 m below the surface at site XD corresponding to the maximum active layer thickness and deepest injection depth. This active layer thickness is far deeper than previously reported for the Arctic (Blume-Werry et al., 2019; Finger et al., 2016; Riley et al., 2018) and critical for plants living on the Tibetan Plateau in order to benefit from N released from thaw permafrost. These observations suggest that plants potentially can utilize nitrogen in the form of ammonium near the permafrost table, and that thawing permafrost therefore can be an important source of NH_4^+ for plants with long plant roots as previously suggested (Elberling et al., 2010; Salmon et al., 2018). However, observations do not exclude that abiotic

transport processes may also influence the vertical distribution of added N and thus the depth of actual N uptake by plants as further discussed in Hansen and Elberling (2023). We therefore conclude that the relative importance of different transport mechanisms remains unclear but appears to function on a short time scale.

Our field observations of plant species being able to utilize additional N from soils below the main root zone and even near the permafrost table are aligned with previous reports from the Arctic (Keuper et al., 2017; Pedersen et al., 2020). However, it is less well documented how an additional N source below the main root zone related to warming and permafrost thawing can influence plant growth and plant composition. Results from our sites (group A sites) showed a clear response over time with respect to vertical maximum root depth increase ($p < 0.01$) and species composition, while this was not observed for group B sites (Fig. S9). At group A sites with significant permafrost thawing and active layer warming, deep-rooted plant species have significantly increased root length (Fig. 4), which indirectly suggests that despite most roots being near the surface, the capability to utilize N at further depths has increased.

4.3. Climate change and plant community composition

In order to quantify how climate change via AL warming and permafrost thawing can influence plant growth and plant species richness, we have applied a piecewise structural equation model (SEM). This allows us to differentiate between direct and indirect effects on plants including thermal conditions (air temperature, growing degree days, soil temperature at 0–50 cm and 50–100 cm and ALT), water availability (soil moisture at 0–50 cm and 50–100 cm) and soil nutrition ($N–NO_3^-$ and $N–NH_4^+$ concentrations for 0–50 cm, 50–100 cm, 100 cm–permafrost table). The SEM model (Fig. 5) highlights the importance of the maximum root length ($R^2 = 0.76$) over growing degree days ($R^2 = 0.59$) and active layer warming ($R^2 = 0.44$). The change in the maximum length of roots is roughly equally controlled by the active layer warming ($R^2 = 0.66$) and permafrost thaw ($R^2 = 0.68$). The SEM results suggest that N released from thawing permafrost can be an important N source in addition to other N sources within the active layer.

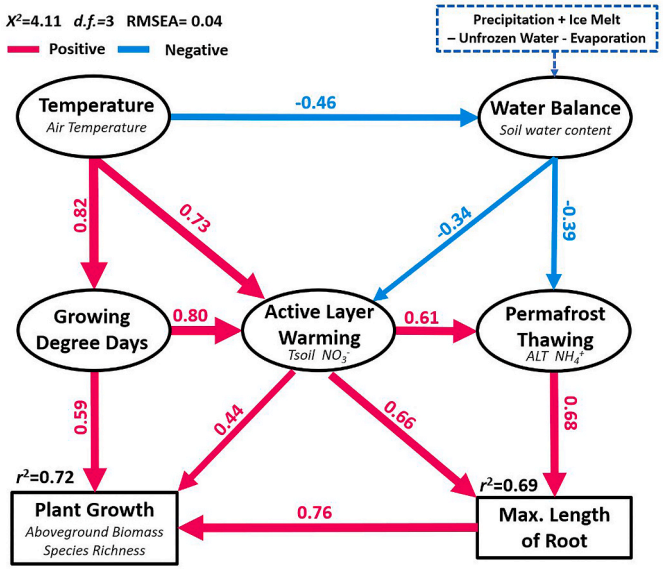

Fig. 5. The structural equation model (SEM) quantifies the direct and indirect pathways of climate change on ecosystem changes, measured as plant growth through additional nitrogen availability due to either active layer warming or permafrost thaw, based on data from group A sites during 1995–2017. The numbers shown by the arrows are the standardized path coefficients and indicate the effect size of the relationship between two variables. Arrow widths are proportional to the path coefficient values. Only significant relationships are shown ($p < 0.05$). Red and blue arrow lines indicate positive and negative relationships, respectively. The chi-square statistic (χ^2), degree of freedom (*d.f.*) and the root-mean-square error of approximation (RMSEA) are shown in the upper left-hand corner of the figure. For more details, please see Supplementary information SI.1.14.

The additional ^{15}N experiment results and the SEM model results combined suggest that deep-rooted plant species benefit from AL warming and permafrost thawing, while shallow-rooted species benefit mainly from GDD. Overall, 72% of plant growth could be explained by maximum root depth, AL warming, and GDD together, whereas 69% of the variation in the maximum root depth could be explained by AL warming and permafrost thawing (Fig. 5).

This result suggests that long-term species composition may depend on how different species benefit from near-surface warming versus permafrost thawing. Also, future grazing by yaks or other large wild animals may influence long-term changes. In this study, all sites were fenced off to avoid grazing by yaks, but grazing by *Ochotona curzoniae* remains an unknown factor, which should be considered in future studies. It is noted that more than 1/3 of the near-surface organic carbon has been mineralized, probably due to climate warming, among other factors, and this has resulted in a major near-surface inorganic N source. The N source linked to thawing permafrost is more complicated, as the source is available at the end of the growing season and the permafrost tables at most sites are below the main root zone.

Overall, the vegetation on the Tibetan Plateau has responded to recent changes in climate (Zhang et al., 2013), but has also been influenced by geography and other factors (Huang et al., 2022). Thus, nitrogen as a nutrient source for increased plant growth and changes in vegetation composition is only one factor among several. This study highlights that despite a deep active layer, thawing permafrost can release inorganic N, which deep-rooted plant species can utilize as an additional source. On the other hand, future work is needed to quantify the importance of permafrost N in relation to other N sources when it comes to the more general vegetation changes observed on the Tibetan Plateau.

Vegetation composition changes and root dynamics in permafrost regions have important additional implications for ecosystem C cycling (Blume-Werry et al., 2019). The increase in root length, root exudates and litter input may provide more C and N under warmer conditions (Salmon et al., 2018; Blume-Werry et al., 2019). The marked increase in the SOC content of the 50–100 cm layer and the change in the C/N ratio at group A sites suggest that changes in vertical root distribution could lead to additional root litter in the 50–100 cm layer and thereby explain an increase in SOC.

5. Conclusion

We conclude that (1) the permafrost samples collected contained higher levels of ammonium than the active layer and that ammonium is released upon thaw; (2) permafrost thaw with corresponding released ammonium can be an important source of inorganic nitrogen; (3) active layer warming has resulted in correspondingly enhanced soil organic matter mineralization within the top 50 cm; (4) permafrost thaw and active layer warming in combination have led to significant changes in plant species composition and growth; (5) the SEM analysis indicates that changes in climate affect both permafrost thaw and active layer warming and thereby explain 69% of the observed changes in maximum root depth and 72% of the observed changes in plant growth.

The combination of labelled ammonium addition (^{15}N), repeated field drilling and plant survey and SEM analysis revealed important links between changes in nitrogen availability and increase in the maximum root depth, which suggest that the vegetation has benefitted from new nitrogen sources and has affected species composition and plant growth. Such changes are expected to have important long-term implications for the ecosystem and people living on the world's highest land.

Declaration of competing interest

The authors declare that they have no known competing financial interests or personal relationships that could have appeared to influence the work reported in this paper.

Data availability

Data will be made available on request.

Acknowledgements

BE and HY were supported by the Danish National Research Foundation (CENPERM DNRF 100). In addition, QB was supported by the National Natural Science Foundation of China (42230512), JT by the Swedish Formas grant (no. 2016-01580), Qing Zhu by the U.S. Department of Energy Reducing Uncertainties in Biogeochemical Interactions through Synthesis and Computation (RUBISCO), W. Z. by the Swedish Research Council VR (2020–05338) and Swedish National Space Agency (209/19), HB was supported by the Chinese Academy of Sciences (YJKYYQ20190012 and E229060201) and State Key Laboratory of Frozen Soil Engineering (SKLFSE-ZT-202111). We thank Anping Chen and Yiqi Luo for their suggestions about the experiment design. We thank Yongzhi Liu, Huijun Jin, Chao Mao, Guojun Liu, and Guilong Wu for field soil sample processing and laboratory analyses. We also thank Licheng Liu and Youmi Oh for aiding with the structure equation model. In addition, our gratitude goes to Sebastian Zastruzny, Laura Helene Rasmussen, Emily P. Pedersen, Anne Christine Krull Pedersen, and Lena Hermesdorf for providing comments on the data analysis. Finally, we would like to acknowledge the very helpful comments from two journal reviewers.

Appendix A. Supplementary data

Supplementary data to this article can be found online at https://doi.org/10.1016/j.soilbio.2023.109041.

References

Beermann, F., et al., 2017. Permafrost thaw and liberation of inorganic nitrogen in Eastern Siberia. Permafrost and Periglacial Processes 28, 605–618. https://doi.org/10.1002/ppp.1958.

Bendixen, M., et al., 2017. Delta progradation in Greenland driven by increasing glacial mass loss. Nature (London) 550, 101–104. https://doi.org/10.1038/nature23873.

Bjorkman, A.D., et al., 2018. Plant functional trait change across a warming tundra biome. Nature (London) 562, 57–62. https://doi.org/10.1038/s41586-018-0563-7.

Blume-Werry, G., Milbau, A., Teuber, L.M., Johansson, M., Dorrepaal, E., 2019. Dwelling in the deep-strongly increased root growth and rooting depth enhance plant interactions with thawing permafrost soil. New Phytologist 223, 1328–1339. https://doi.org/10.1111/nph.15903.

Chen, D., et al., 2015. Assessment of past, present and future environmental changes on the Tibetan Plateau. Chinese Science Bulletin 60, 3025–3035. https://doi.org/10.1360/N972014-01370.

Clemmensen, K.E., et al., 2008. Site-dependent N uptake from N-form mixtures by arctic plants, soil microbes and ectomycorrhizal fungi. Oecologia 155, 771–783. https://doi.org/10.1007/s00442-008-0962-9.

Ehlers, T.A., Chen, D., Appel, E.T., et al., 2022. Past, present, and future geo-biosphere interactions on the Tibetan Plateau and implications for permafrost. Earth-Science Reviews, 104197. https://doi.org/10.1016/j.earscirev.2022.104197.

Elberling, B., Christiansen, H.H., Hansen, B.U., 2010. High nitrous oxide production from thawing permafrost. Nature Geoscience 3, 332–335. https://doi.org/10.1038/ngeo803.

Elmendorf, S.C., et al., 2012. Plot-scale evidence of tundra vegetation change and links to recent summer warming. Nature Climate Change 2, 453–457. https://doi.org/10.1038/nclimate1465.

Finger, R.A., et al., 2016. Effects of permafrost thaw on nitrogen availability and plant-soil interactions in a boreal Alaskan lowland. Journal of Ecology 104, 1542–1554. https://doi.org/10.1111/1365-2745.12639.

Grace, J.B., 2006. Structural Equation Modeling and Natural Systems. Cambridge University Press.

Hansen, H.F.E., Elberling, B., 2023. Spatial distribution of bioavailable inorganic nitrogen from thawing permafrost. Global Biogeochemistry Cycles 37, e2022GB007589. https://doi.org/10.1029/2022GB007589.

Happonen, K., Virkkala, A.M., Kemppinen, J., Niittynen, P., Luoto, M., 2022. Relationships between above-ground plant traits and carbon cycling in tundra plant communities. Journal of Ecology 110, 700–716. https://doi.org/10.1111/1365-2745.13832.

Heijmans, M.M., et al., 2022. Tundra vegetation change and impacts on permafrost. Nature Reviews Earth & Environment 3, 68–84. https://doi.org/10.1038/s43017-021-00233-0.

Hewitt, R.E., Taylor, D.L., Genet, H., McGuire, A.D., Mack, M.C., 2019. Below-ground plant traits influence tundra plant acquisition of newly thawed permafrost nitrogen. Journal of Ecology 107, 950–962. https://doi.org/10.1111/1365-2745.13062.

Huang, Y., et al., 2022. Tibetan Plateau greening driven by warming-wetting climate change and ecological restoration in the 21st century. Land Degradation & Development 33, 2407–2422. https://doi.org/10.1002/ldr.4319.

Iversen, C.M., et al., 2015. The unseen iceberg: plant roots in arctic tundra. New Phytologist 205, 34–58. https://doi.org/10.1111/nph.13003.

Keuper, F., et al., 2017. Experimentally increased nutrient availability at the permafrost thaw front selectively enhances biomass production of deep-rooting subarctic peatland species. Global Change Biology 23, 4257–4266. https://doi.org/10.1111/gcb.13804.

Kou, D., et al., 2020. Progressive nitrogen limitation across the Tibetan alpine permafrost region. Nature Communications 11, 3331. https://doi.org/10.1038/s41467-020-17169-6.

Liu, H., et al., 2018. Shifting plant species composition in response to climate change stabilizes grassland primary production. Proceedings of the National Academy of Sciences of the United States of America 115, 4051–4056. https://doi.org/10.1073/pnas.1700299114.

Mallet, A.A., 1986. A maximum likelihood estimation method for random coefficient regression models. Biometrika 73, 645–656. https://doi.org/10.1093/biomet/73.3.645.

McNamara, J.P., Kane, D.P., Hinzman, L.D., 1999. An analysis of an arctic channel network using a digital elevation model. Geomorphology 29, 339–353. https://doi.org/10.1016/S0169-555X(99)00017-3.

Myers-Smith, I.H., et al., 2019. Eighteen years of ecological monitoring reveals multiple lines of evidence for tundra vegetation change. Ecological Monographs 89, e01351. https://doi.org/10.1002/ecm.1351.

Niittynen, P., Heikkinen, R.K., Luoto, M., 2018. Snow cover is a neglected driver of Arctic biodiversity loss. Nature Climate Change 8, 997–1001. https://doi.org/10.1038/s41558-018-0311-x.

Obu, J., et al., 2019. Northern Hemisphere permafrost map based on TTOP modelling for 2000–2016 at 1 km^2 scale. Earth-Science Reviews 193, 299–316. https://doi.org/10.1016/j.earscirev.2019.04.023.

Oulehle, F., et al., 2016. Plant functional type affects nitrogen use efficiency in high-Arctic tundra. Soil Biology and Biochemistry 94, 19–28. https://doi.org/10.1016/j.soilbio.2015.11.008.

Parmesan, C., et al., 2022. Terrestrial and freshwater ecosystems and their services. In: Pörtner, H.-O., et al. (Eds.), *Climate Change 2022: Impacts, Adaptation, and Vulnerability*. Contribution of Working Group II to the Sixth Assessment Report of the Intergovernmental Panel on Climate Change. Cambridge University Press.

Pedersen, E.P., Elberling, B., Michelsen, A., 2020. Foraging deeply: depth-specific plant nitrogen uptake in response to climate-induced N-release and permafrost thaw in the High Arctic. Global Change Biology 26 (11), 6523–6536. https://doi.org/10.1111/gcb.15306.

Pedersen, E.P., Elberling, B., Michelsen, A., 2022. Upslope release – downslope receipt? Multi-year plant uptake of permafrost-released nitrogen along an arctic hillslope. Journal of Ecology 110, 1896–1912. https://doi.org/10.1111/1365-2745.13925.

Riley, W.J., Zhu, Q., Tang, J.Y., 2018. Weaker land-climate feedbacks from nutrient uptake during photosynthesis-inactive periods. Nature Climate Change 8, 1002–1006. https://doi.org/10.1038/s41558-018-0325-4.

Salmon, V.G., et al., 2018. Adding depth to our understanding of nitrogen dynamics in permafrost soils. Journal of Geophysical Research and Biogeosciences 123, 2497–2512. https://doi.org/10.1029/2018JG004518.

Schuur, E.A., Crummer, K.G., Vogel, J.G., Mack, M.C., 2007. Plant species composition and productivity following permafrost thaw and thermokarst in Alaskan tundra. Ecosystem 10, 280–292. https://doi.org/10.1007/s10021-007-9024-0.

Thomas, H.J., et al., 2020. Global plant trait relationships extend to the climatic extremes of the tundra biome. Nature Communications 11, 1–12. https://doi.org/10.1038/s41467-020-15014-4.

Virkkala, A.M., et al., 2021. Statistical upscaling of ecosystem CO_2 fluxes across the terrestrial tundra and boreal domain: regional patterns and uncertainties. Global Change Biology 27, 4040–4059. https://doi.org/10.1111/gcb.15659.

Wang, T., et al., 2020. Permafrost thawing puts the frozen carbon at risk over the Tibetan Plateau. Science Advances 6. https://doi.org/10.1126/sciadv.aaz3513 eaaz3513.

Wu, X., et al., 2016. Environmental controls on soil organic carbon and nitrogen stocks in the high-altitude arid western Qinghai-Tibetan Plateau permafrost region. Journal of Geophysical Research and Biogeosciences 121, 176–187. https://doi.org/10.1002/2015JG003138.

Yao, T., et al., 2019. Recent third pole's rapid warming accompanies cryospheric melt and water cycle intensification and interactions between monsoon and environment: multidisciplinary approach with observations, modelling, and analysis. Bulletin of the American Meteorological Society 100, 423–444. https://doi.org/10.1175/BAMS-D-17-0057.1.

Yun, H., et al., 2018. Consumption of atmospheric methane by the Qinghai–Tibet Plateau alpine steppe ecosystem. Cryosphere 12, 2803–2819. https://doi.org/10.5194/tc-12-2803-2018.

Zhang, G., et al., 2013. Green-up dates in the Tibetan Plateau have continuously advanced from 1982 to 2011. Proceedings of the National Academy of Sciences of the United States of America 110, 4309–4314. https://doi.org/10.1073/pnas.1210423110.

Zou, D., et al., 2017. A new map of permafrost distribution on the Tibetan Plateau. Cryosphere 11 (6), 2527–2542. https://doi.org/10.5194/tc-11-2527-2017.